Human Molecular Genetics, 2012, Vol. 21, No. 1 **185–195**
doi:10.1093/hmg/ddr453
Advance Access published on October 3, 2011

Severe neuromuscular denervation of clinically relevant muscles in a mouse model of spinal muscular atrophy

Karen K. Y. Ling[†], Rebecca M. Gibbs[†], Zhihua Feng and Chien-Ping Ko[*]

Section of Neurobiology, Department of Biological Sciences, University of Southern California, Los Angeles, CA 90089-2520, USA

Received August 8, 2011; Revised September 9, 2011; Accepted September 27, 2011

Spinal muscular atrophy (SMA), a motoneuron disease caused by a deficiency of the survival of motor neuron (SMN) protein, is characterized by motoneuron loss and muscle weakness. It remains unclear whether widespread loss of neuromuscular junctions (NMJs) is involved in SMA pathogenesis. We undertook a systematic examination of NMJ innervation patterns in >20 muscles in the SMNΔ7 SMA mouse model. We found that severe denervation (<50% fully innervated endplates) occurs selectively in many vulnerable axial muscles and several appendicular muscles at the disease end stage. Since these vulnerable muscles were located throughout the body and were comprised of varying muscle fiber types, it is unlikely that muscle location or fiber type determines susceptibility to denervation. Furthermore, we found a similar extent of neurofilament accumulation at NMJs in both vulnerable and resistant muscles before the onset of denervation, suggesting that neurofilament accumulation does not predict subsequent NMJ denervation. Since vulnerable muscles were initially innervated, but later denervated, loss of innervation in SMA may be attributed to defects in synapse maintenance. Finally, we found that denervation was amendable by trichostatin A (TSA) treatment, which increased innervation in clinically relevant muscles in TSA-treated SMNΔ7 mice. Our findings suggest that neuromuscular denervation in vulnerable muscles is a widespread pathology in SMA, and can serve as a preparation for elucidating the biological basis of synapse loss, and for evaluating therapeutic efficacy.

INTRODUCTION

Proximal spinal muscular atrophy (SMA) is a motoneuron disease caused by the homozygous deletion/mutation of the *Survival of Motor Neuron* (*SMN*) *1* gene (1), resulting in a deficiency of the ubiquitously expressed SMN protein, which may play a role in snRNP biogenesis (2–4). Since patients always retain several copies of the closely related *SMN2* gene, which only produces low levels of functional full-length SMN, the copy number of *SMN2* modifies disease severity (5–7). Infants with severe SMA experience proximal muscle weakness in axial muscles that stabilize the trunk and head and have shortened life expectancies due to compromised vital motor functions, such as breathing and swallowing (8). The key pathogenic events of this devastating disorder remain unclear (2,9), and since there are no effective treatment options, SMA remains the most frequent genetic cause of infant mortality (10,11).

Clinical studies have suggested that muscle weakness may be due to neuromuscular junction (NMJ) denervation as demonstrated by reduced motor unit number estimates and maximum compound muscle action potentials (12). Studies in various SMA mouse models have shown abnormalities of NMJs, including neurofilament accumulation at presynaptic terminals, smaller and immature endplates, as well as reduced transmitter release (13–19). However, NMJs in several distal hindlimb muscles are fully innervated in the widely used SMNΔ7 SMA mouse line, even at the disease end stage (15,17,20). Despite a reduction in transmitter release at the presynaptic terminal (15,17), no transmission failures were observed in hindlimb NMJs (17,20) to account for the motor deficit. It was shown recently that hindlimb

[*]To whom correspondence should be addressed. Tel: +1 2137409182; Fax: +1 2137405687; Email: cko@dornsife.usc.edu
[†]The authors wish it to be known that, in their opinion, the first two authors should be regarded as joint First Authors.

motor impairment may instead be attributed to synaptic defects in lumbar spinal motoneurons (17,21,22).

Given the profound proximal weakness observed in SMA patients, studies have also focused on NMJs in proximal regions. Recent studies of a severe SMA mouse model (Smn−/−;SMN2) revealed that although NMJs were formed at birth, abnormal neurofilament accumulation and denervation (>65% fully innervated) occurred in several axial muscles (e.g. levator auris longus, transversus abdominis, auricularis superior, intercostal) at the disease end stage [postnatal day 5 (P5)] (18,23,24). These studies suggest that NMJ denervation in a subset of muscles may contribute to muscle weakness in Smn−/−;SMN2 mice. However, in the slightly less severe SMA mouse model (SMNΔ7), these vulnerable muscles (i.e. levator auris longus, transversus abdominis, paraspinal) were reported to have much milder NMJ denervation (>80% fully innervated) (15,18). It remains unclear whether and how widespread NMJ loss contributes to motor impairment in the milder SMNΔ7 mice.

Given the fact that SMNΔ7 mice have an extended lifespan of ∼2 weeks, which provides an ideal platform for assessing therapeutic efficacy, a thorough and systematic investigation of NMJ loss in SMNΔ7 mice would necessitate preclinical drug testing. In addition, such a study would promote an understanding of the progression of NMJ loss, and would also provide a foundation for understanding potential factors contributing to the selective vulnerability of NMJs in SMA (e.g. muscle location, fiber types, innervating motoneuron pools or synapsing phenotypes).

In the current study, we undertook a systematic investigation of NMJs in a wide range of axial (head, neck and trunk) and appendicular (controlling the limb) muscles that are relevant to SMA symptomatology. We found that severe denervation, attributed to defects in synapse maintenance, is a significant pathological event occurring in a wide range of SMNΔ7 muscles. Furthermore, we found that selective NMJ loss is not predicted by muscle location, muscle fiber types or neurofilament accumulation at the motor nerve terminal. To validate this severe denervation as a preparation for drug efficacy studies, we treated SMNΔ7 mice with trichostatin A (TSA), which has previously been shown to increase SMN expression and life span in this mouse model (25). We found that denervation was mitigated by pharmacological intervention with TSA. Therefore, these severely denervated muscles can serve as excellent preparations for elucidating potential mechanisms driving selective denervation and for preclinical testing of drug efficacy in alleviating neuromuscular defects.

RESULTS

Severe denervation in clinically relevant muscles of SMNΔ7 mice at the disease end stage

To establish which muscles are highly vulnerable to denervation in SMA, we have examined NMJ innervation patterns in >20 different axial muscles (head, neck and trunk) and proximal and distal appendicular muscles (controlling the limbs) from SMNΔ7 mice at the disease end stage (around P14). To facilitate the visualization of NMJs, we labeled motor endplates with α-bungarotoxin and immunostained nerve terminals with anti-synaptophysin antibodies in a SMNΔ7 mouse line that expresses yellow fluorescent protein (YFP) in motoneurons (17). Figure 1A shows examples of double-labeled NMJs of the resistant and vulnerable muscles in P14 SMNΔ7 mice. Endplates (in yellow) in the resistant muscles were all fully innervated as shown by the overlapping nerve terminals (in green) and acetylcholine receptor (AChR) clusters (in red). In contrast, not all endplates were innervated in the vulnerable muscles as shown by the presence of unoccupied endplates (AChR clusters without overlying nerve terminals in Fig. 1A; a magnified view of NMJs shown in Fig. 1B). The percentage of fully innervated endplates in a wide range of proximal and distal muscles in SMNΔ7 end-stage mice compared with non-SMA control littermates was quantified in Figure 2. Our results revealed a group of axial and appendicular muscles that display severe denervation (<50% of endplates remain fully innervated). It is important to note that a number of these vulnerable muscles are essential for functions that are affected in SMA patients, including the splenius capitis, longissimus capitis and semispinalis capitis muscles that are responsible for head posture and movement, the serratus posterior inferior (SPI) muscle that is involved in respiratory function, and the masseter and sternohyoid muscles that are involved in mastication and swallowing (26). However, whether these muscles are denervated in SMA patients has not been determined. Aside from these axial muscles, we have also observed NMJ denervation in some appendicular muscles located in the proximal limb (i.e. triceps) and distal limb [i.e. flexor digitorum brevis (FDB)]. Among all the appendicular muscles examined, the FDB muscle of the hindpaw was the most severely denervated (Fig. 1A). The FDB is anatomically divided into three slender muscles which flex the second, third and fourth digits upon contraction (27). Interestingly, only the FDB-2 and -3 (muscle branches with separate tendons inserted to the second and third phalanges, respectively) were significantly denervated, whereas the FDB-4 (muscle branches inserted to the fourth phalanx) was fully innervated (Figs 1A and 2). This result supports the idea that muscle vulnerability to denervation is not necessarily dependent upon muscle location or function.

Together, we found denervation in a majority of axial muscles and a few appendicular muscles in end-stage SMNΔ7 mice. The severe denervation in a series of head and trunk muscles in SMNΔ7 mice might compromise vital motor functions, which are clinically relevant to SMA patients. Furthermore, our data suggest that NMJs in axial muscles are generally more vulnerable to denervation, but there is no simple correlation between NMJ vulnerability and muscle location or proximity to the spine.

Denervation results from failures in synapse maintenance in SMNΔ7 mice

NMJ denervation in the severe SMA mouse model (Smn−/−;SMN2) has been shown to occur as a failure of synaptic maintenance (23,24). To investigate whether denervation in vulnerable muscles in the SMNΔ7 mouse model is also due to a failure of synaptic maintenance or a lack of initial nerve-muscle contact, we characterized the time

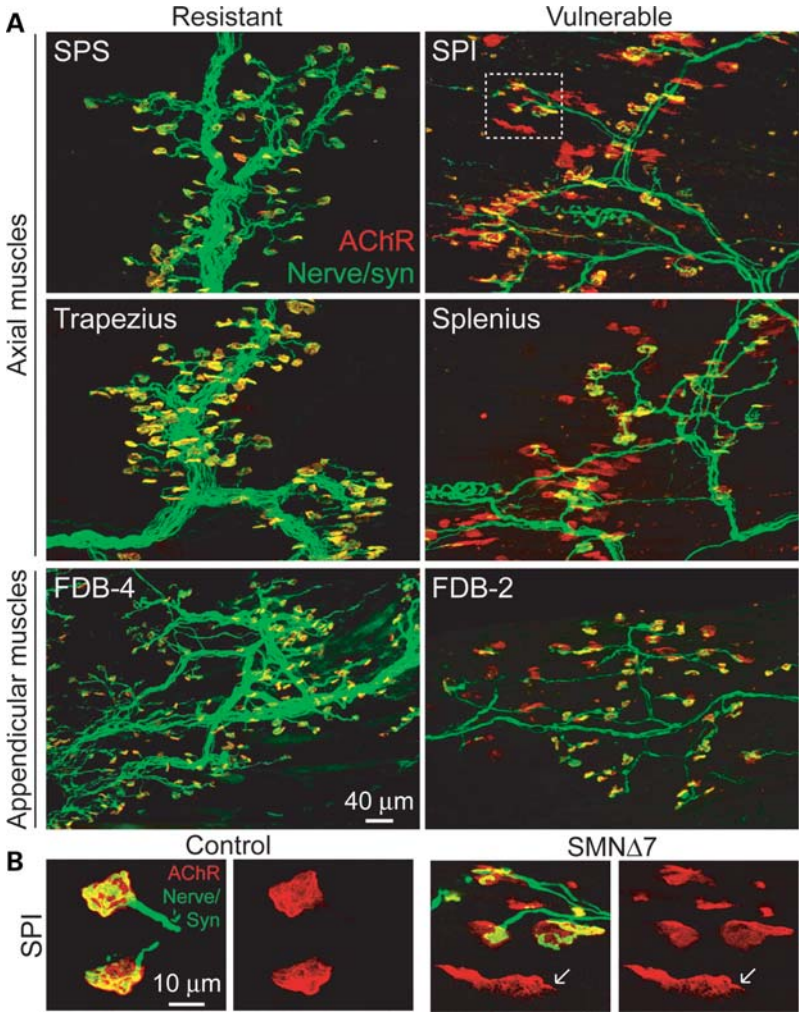

Figure 1. Severe denervation of proximal and distal muscles in end-stage SMNΔ7 mice. (**A**) Axial muscles [serratus posterior superior (SPS), SPI, trapezius and splenius] and appendicular muscles (FDB-4 and -2) of YFP-SMA mice were immunostained for nerve terminals with anti-synaptophysin [syn] (in green) and motor endplates with α-bungarotoxin (in red). (**B**) Selected high-magnification images of NMJs in SPI muscles of control and SMNΔ7 mice at P14. Arrows indicate dispersing AChR clusters at a denervated endplate in SMNΔ7 mice.

course of denervation in the SPI, a severely denervated axial muscle, and the most severely denervated appendicular muscle, FDB-2/3.

In the SPI muscles at embryonic day (E) 17.5, we found that almost all endplates were fully innervated by nerve terminals (labeled with anti-neurofilament and anti-synaptophysin in Fig. 3A) in both control and SMNΔ7 mice. The percentage of innervation was quantified in Figure 3B (SMNΔ7: 98.1 ± 0.8%, 749 NMJs, $n = 3$ animals versus control: 96.1 ± 1.2%, 502 NMJs, $n = 3$ animals). However, at around birth (E19.5–P1), only ∼45% of endplates in the SMNΔ7 SPI were fully innervated by nerves (Fig. 3A and B; E19.5: 48.7 ± 13%, 940 NMJs, $n = 4$ animals; P1: 45.5 ± 20.1%, 702 NMJs, $n = 3$ animals), while the remaining endplates were either fully denervated (E19.5: 38.3 ± 5%; P1: 36.5 ± 11.7%) or partially denervated (E19.5: 13.0 ± 4.2%; P1:18 ± 8.6%) (Fig. 3C). Similarly, unoccupied endplates were also observed in other vulnerable muscles (e.g. longissimus, splenius, semispinalis and triceps) at P1 (data not shown). Further NMJ loss in the SMNΔ7 SPI occurred over the next 3 days and at P4, only ∼13.2 ± 5.5% (1121 NMJs, $n = 4$ animals) of endplates remained fully innervated (Fig. 3B). There was no further loss of innervation beyond this age. This result implies that SMNΔ7 neurons are capable of initially finding their synaptic targets and forming synapses. However, these synaptic contacts are not maintained and are lost rapidly during the disease progression.

In the vulnerable appendicular FDB-2/3 muscle, we found that initial NMJ formation is also not affected as evidenced by the observation that almost all motor endplates were fully co-localized with the presynaptic marker, synaptophysin, at P1 (Fig. 4A). However, at P4, we began to observe partially (11.5 ± 14.1%) and completely (7.5 ± 10.5%) denervated endplates in SMNΔ7 FDB-2/3 muscles (Fig. 4C). Denervation then progressed rapidly in these muscles within the first week of life (Fig. 4B and C). At P7, significant denervation was observed and only 31.6 ± 10.5% of NMJs remained fully innervated at this time point (779 NMJs, $n = 3$ animals). There was no further loss of innervation between P7 and the disease end stage (Fig. 4B and C). These results further

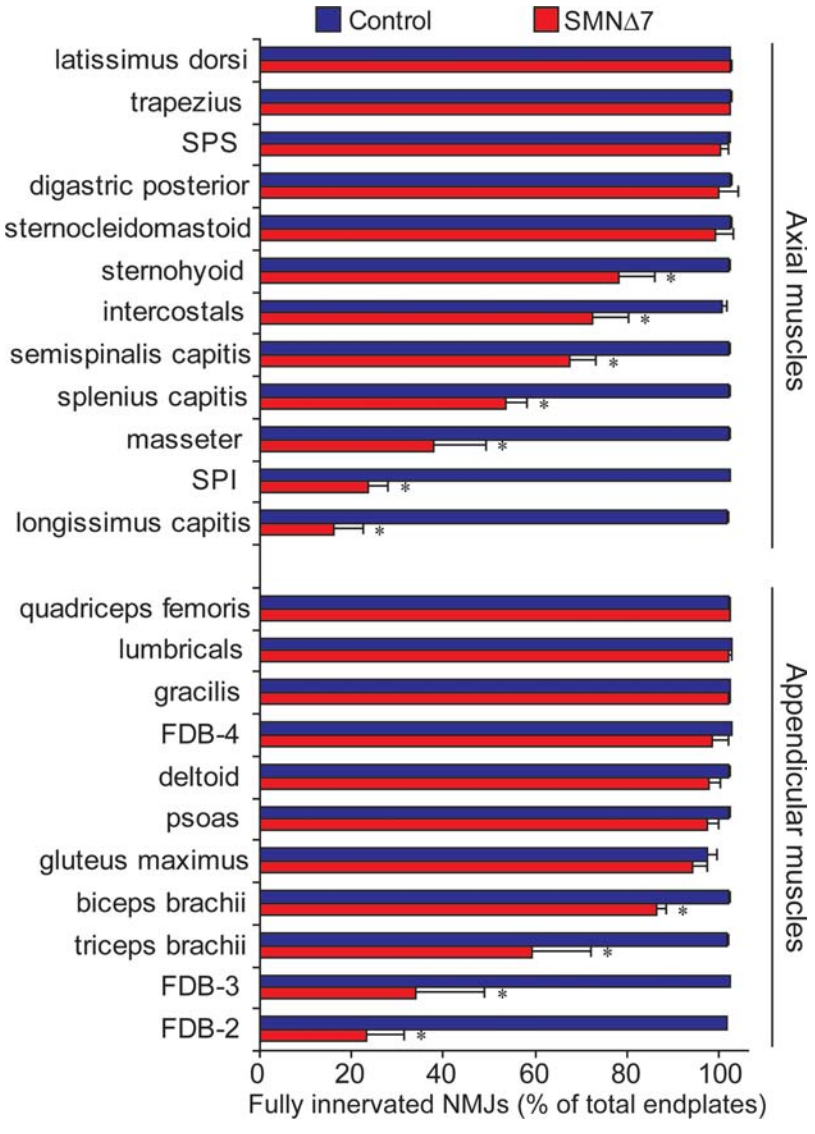

Figure 2. Quantitative analyses of innervation in a wide range of axial and appendicular muscles in end-staged (P12–14) SMNΔ7 mice and age-matched control mice. Axial and appendicular muscles were immunostained for nerve terminals with anti-synaptophysin and motor endplates with α-bungarotoxin. Innervation percentage was expressed as the number of fully innervated endplates over the total number of analyzed endplates (>200 NMJs) in each animal. The average percentage was obtained from three to five pairs of animals. Data are expressed as mean ± SEM. $^{*}P < 0.05$.

suggest that nerve-muscle contacts are able to initially form, but are not maintained in the vulnerable branches of the FDB.

Developing NMJs are multiply innervated at birth (28). To confirm that there is no defect in synapse formation, we examined the number of presynaptic inputs per endplate before the onset of denervation. We found that the average number of axonal inputs in the SMNΔ7 FDB-2 was not significantly different from that of control FDB-2 muscles at P1 (Fig. 4D). In addition, the number of axonal inputs in the vulnerable (FDB-2) muscles was similar to that in the resistant (FDB-4) muscles at the same time point (Fig. 4D). This suggests that there is no developmental defect in initial nerve innervation of endplates in vulnerable muscles to differentiate them from the resistant muscles. Together, our data suggest that denervation in vulnerable muscles in SMNΔ7 mice likely results from deficits in synapse maintenance, rather than formation.

Presynaptic pathology is observed in muscles regardless of their vulnerability to denervation

Neurofilament accumulation in the axonal swellings and at the presynaptic terminal is considered one of the morphological hallmarks of NMJs in SMA mice and patients (13–15,18,24,29). To investigate whether or not this presynaptic pathology predicts NMJ vulnerability to denervation, we examined and compared the percentage of NMJs with neurofilament accumulation in vulnerable (FDB-2) and resistant (FDB-4) muscles before and after denervation. At P1 (before any denervation occurs), we already observed neurofilament accumulation (indicated by arrowheads) in the vulnerable FDB-2 muscles in SMNΔ7 mice (Fig. 5A). However, the percentage of NMJs displaying neurofilament accumulation in the vulnerable FDB-2 (36.8 ± 5.8%) muscle was not significantly different from that of resistant FDB-4 (28.13 ± 9.2%) muscles

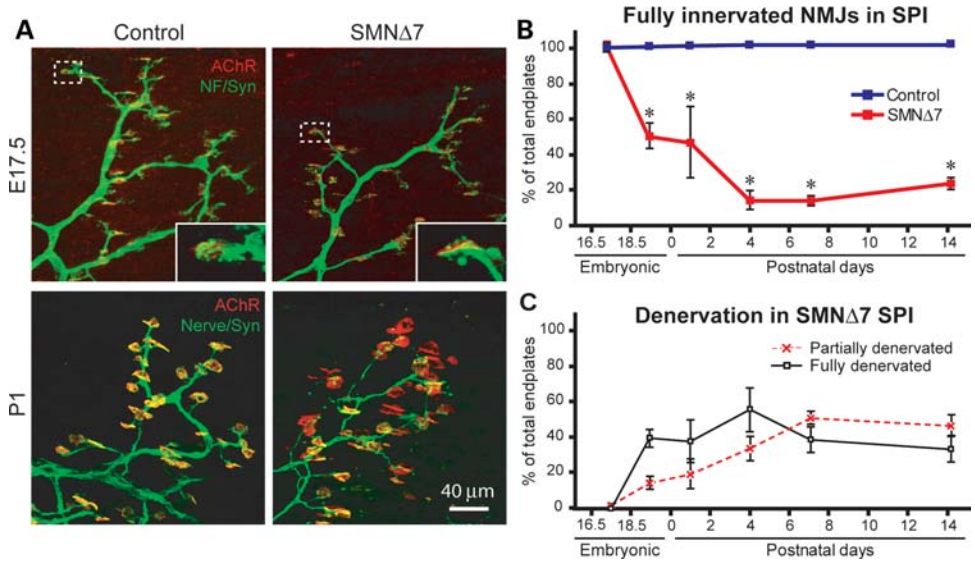

Figure 3. NMJs are formed but not maintained in the vulnerable axial muscle, SPI, in SMNΔ7 mice. (**A**) Sample immunomicrographs showing NMJs in whole-mount SPI muscles of control and SMNΔ7 mice at E17.5 and P1. NMJs were labeled for nerves with either anti-neurofilament antibody or YFP-nerve (in green) and with anti-synaptophysin antibody. Endplates were labeled with α-bungarotoxin (in red). Insets are magnified views of sample NMJs at E17.5. (**B**) Quantification of fully innervated endplates in the SPI of control and SMNΔ7 mice during development (E17.5–P14). (**C**) Quantification of partially or fully denervated endplates in SPI muscles of SMNΔ7 mice during E17.5–P14. All quantitative data are expressed as mean ± SEM. $^*P < 0.05$.

in P1 SMNΔ7 mice (Fig. 5B, $n = 3$ animals). Even at P14, the percentage of innervated NMJs displaying neurofilament accumulation increased to a similar extent in both vulnerable FDB-2 (87.4 ± 6.4%) and resistant FDB-4 (95.4 ± 2.7%) in SMNΔ7 mice (Fig. 5B). This result suggests that the pathological accumulation of neurofilament at nerve terminals does not correlate with NMJ vulnerability to subsequent denervation.

Denervation in clinically relevant muscles is ameliorated by TSA treatment

To investigate whether denervation in vulnerable muscles can serve as a reliable marker for evaluating drug efficacy at the NMJ, we treated SMNΔ7 mice from P1 to P12 with daily intraperitoneal (IP) injections (10 mg/kg body weight) of TSA, a histone deacetylase inhibitor that has previously been shown to upregulate SMN expression, improve motor deficits and increase lifespan in SMNΔ7 mice (25). For a control, we administered daily IP injections of vehicle [dimethyl sulfoxide (DMSO)] to SMNΔ7 littermates, using equal volumes of vehicle and TSA solutions. After 2 weeks of drug treatment, we chose to examine the NMJ innervation pattern in several clinically relevant muscles that are severely denervated in SMNΔ7 end-stage mice, including the longissimus capitis, splenius capitis, SPI and semispinalis capitis. Overall, we found that the vulnerable muscles of SMNΔ7 mice that were treated daily with TSA had an average 28.9% increase in the number of fully innervated NMJs at P12 when compared with control SMNΔ7 littermates injected daily with DMSO (Fig. 6). For example, in the longissimus capitis, TSA treatment resulted in a ∼3-fold increase in the number of fully innervated endplates (vehicle: 14.7 ± 10.9% versus TSA: 43.1 ± 12.9%). Similarly, in the splenius capitis, we observed a ∼2-fold increase (vehicle: 33.3 ± 14.6% versus TSA: 64.3 ± 9.6%). We also observed a significant increase in other vulnerable muscles, including the SPI (vehicle: 34.9 ± 3.2% versus treated: 46.6 ± 10.4%) and semispinalis (vehicle: 58.4 ± 9.5% versus treated: 76.0 ± 1.8%). More strikingly, the amount of fully denervated endplates in these vulnerable muscles was reduced by ∼90% in TSA-treated mice when compared with vehicle-treated controls (Fig. 6). Furthermore, we also observed increases in the body weights of TSA-treated mice compared with control littermates (data not shown) that are consistent with findings from previous studies and indicate the successful upregulation of SMN in TSA-treated mice (25). Our results suggest that the progression of NMJ denervation can be ameliorated given an effective pharmaceutical intervention. These severely denervated vulnerable muscles of SMNΔ7 mice, which are clinically relevant to SMA patient symptoms, can serve as novel *in vivo* preparations for evaluating drug efficacy.

DISCUSSION

Our study generates several important findings that promote a better understanding of neuromuscular pathology during the course of SMA. First, we uncovered severe denervation in many muscles involved in vital motor functions (e.g. maintaining head posture, respiration, mastication) in end-stage SMNΔ7 mice. Secondly, we found that denervation is more prominent in muscles located in the head and trunk, but denervation also occurred in proximal and distal limb muscles. Thus, NMJ vulnerability is not solely determined by muscle location. Thirdly, we demonstrated that the loss of innervation likely results from defects in synapse maintenance rather than initial formation of nerve-muscle contacts. Fourthly, presynaptic pathology (i.e. neurofilament

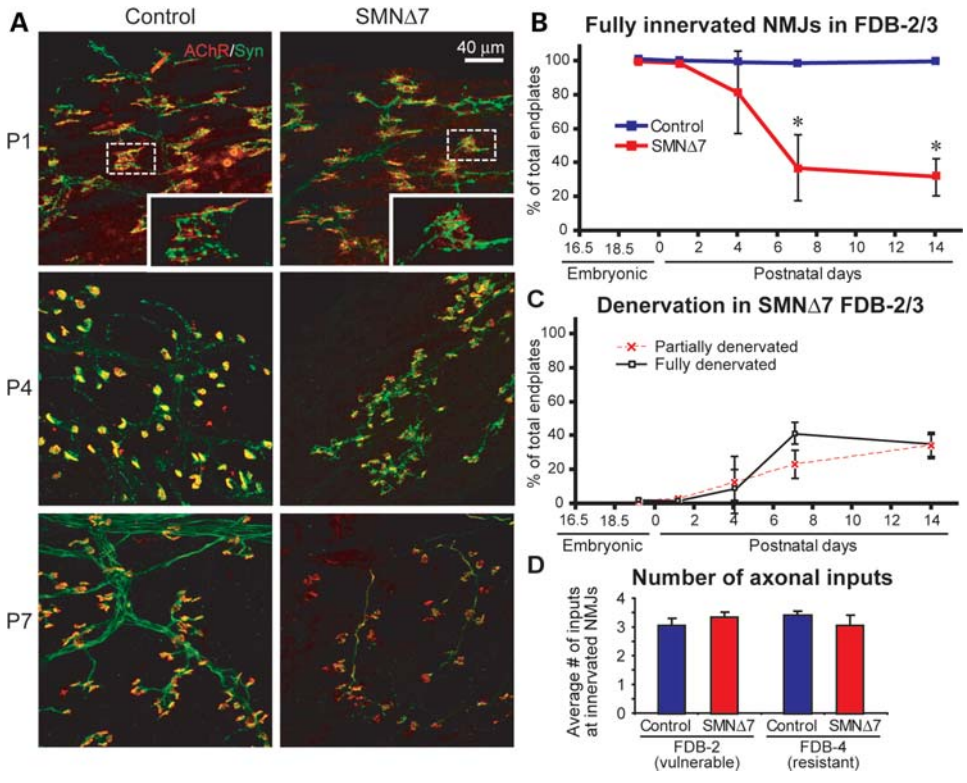

Figure 4. NMJs are formed but not maintained in the vulnerable appendicular muscle, FDB-2/3, in SMNΔ7 mice. (**A**) Sample immunomicrographs of the control and SMNΔ7 FDB-2 muscles at P1, P4 and P7. NMJs were immunostained for nerve terminals with anti-synaptophysin (in green) and endplates with α-bungarotoxin (in red). Insets are magnified views of sample NMJs. (**B**) Quantification of fully innervated endplates in FDB-2/3 muscles of control and SMNΔ7 mice during postnatal development (E19.5–P14). (**C**) Quantification of partially or fully denervated endplates in SMNΔ7 FDB-2/3 muscles during E19.5–P14. (**D**) Quantification of the number of presynaptic inputs (labeled by anti-neurofilament) at the vulnerable FDB-2 muscle and the resistant FDB-4 muscles in the control and SMNΔ7 mice at P1. All quantitative data are mean ± SEM. $^*P < 0.05$.

accumulation) did not correlate with NMJ vulnerability to denervation. Finally, we demonstrated that severe denervation in clinically relevant muscles is amendable by postnatal TSA treatment in SMNΔ7 mice. Given these findings, it is evident that these severely denervated muscles could serve as an excellent preparation for addressing potential mechanisms of NMJ loss in SMA and for preclinical assessment of drug efficacy in alleviating neuromuscular denervation.

Severe and selective denervation in SMA

Previous findings reported synaptic abnormalities (e.g. neurofilament accumulation and reduction in transmitter release) at NMJs in several hindlimb muscles in SMNΔ7 mice. Despite a significant loss of synaptic inputs onto the innervating motoneurons (17,21), these muscles remained innervated throughout disease progression (15,17,20). Our systematic examination of NMJs in the same mouse model revealed severe denervation occurring in a selective manner. We observed that many vulnerable muscles were located proximal to the spine and denervation took place earlier and in a more widespread manner in proximal compared with distal regions in SMNΔ7 mice. This pattern of selectivity is consistent with the pattern of muscle weakness in human SMA patients (1,8). The current study therefore ascertains the involvement of NMJ denervation in vulnerable muscles in SMNΔ7 mice and highlights the importance of focusing on these muscles when assessing NMJ connectivity in SMA patients.

What contributes to synapse vulnerability in SMA?

Our systematic investigation of synapse loss in many axial and appendicular muscles allowed us to study which factors contribute to synapse vulnerability in SMA, such as the locations of muscles or motoneuron pools, muscle fiber types and synapsing phenotypes.

Our data demonstrated that although axial muscles are generally more vulnerable to denervation, both proximal and distal regions of the SMNΔ7 mouse contain both resistant and vulnerable muscles. These results suggest that muscle location does not necessarily determine NMJ vulnerability. Nonetheless, we noted that the vast majority of vulnerable muscles are innervated by motoneurons located in the cervical and thoracic spinal cord segments (Fig. 7). Whether there is a selective degeneration of cervical and thoracic motoneurons is still in debate (14,30,31). Since motoneurons residing in the same spinal segments innervate both vulnerable and resistant muscle groups, whether or not there is a selective degeneration of motoneurons within the same spinal segments that may account for selective NMJ loss requires further investigation. In addition, it has been shown that a loss of excitatory synapses onto motoneurons may contribute to motor deficits

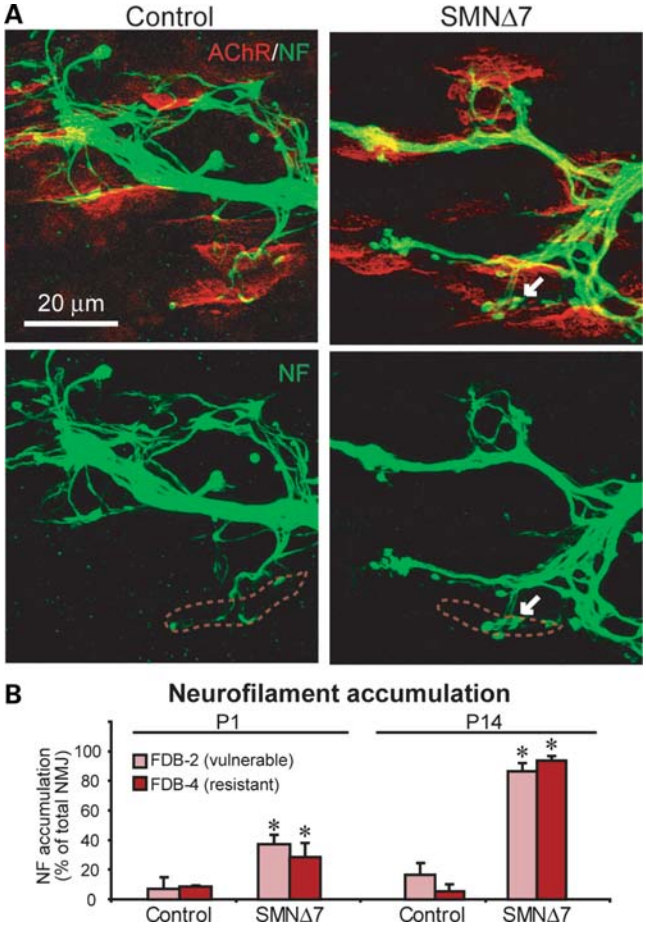

Figure 5. Neurofilament accumulation is observed in both vulnerable and resistant muscles in SMNΔ7 mice at P1 and P14. (**A**) Sample immunomicrographs showing NMJs stained with anti-neurofilament (in green) and endplates with α-bungarotoxin (in red) in FDB-2 muscles in control and SMNΔ7 mice at P1. Arrows indicate an example of neurofilament accumulation at a nerve terminal and red dotted lines outline the endplate region. (**B**) Quantification of the percentage of NMJs that showed neurofilament accumulation in the vulnerable (FDB-2) and resistant (FDB-4) muscles at P1 and P14. All quantitative data are mean ± SEM. $^{*}P < 0.05$.

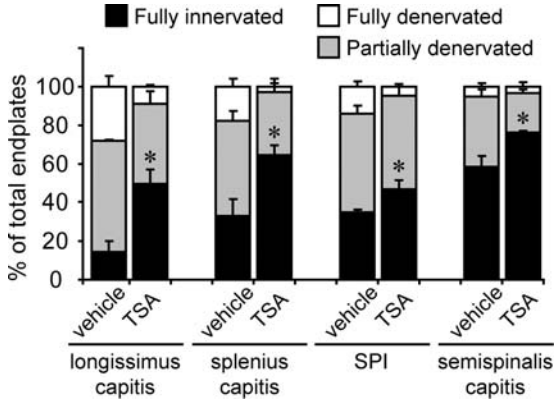

Figure 6. Daily IP injections of TSA mitigated denervation in clinically relevant proximal muscles in SMNΔ7 mice at the end stage (P12–14). Quantification of fully innervated endplates (black bars), partially denervated endplates (gray bars) and fully denervated endplates (white bars) in muscles of vehicle-treated and TSA-treated SMNΔ7 mice at P12–14. All quantitative data are mean ± SEM. $^{*}P < 0.05$.

(17,21,22). It is therefore possible that a selective loss of central synapses may determine selective muscle vulnerability. It would be interesting to study if motoneuron pools innervating vulnerable or resistant muscles are differentially susceptible to central synapse loss. Furthermore, because NMJ loss could occur without motoneuron loss, it would be interesting to investigate in the future whether NMJ denervation in the vulnerable muscles of SMA occurs in a 'dying-back' fashion, as shown in amyotrophic lateral sclerosis (32).

Muscle fiber types have been proposed to render synapse vulnerability in neurodegenerative diseases. Specifically, fast muscle fibers innervated by fast fatigable motoneurons are more vulnerable to denervation in amyotrophic lateral sclerosis (33–35). However, we did not observe a simple correlation between muscle fiber type and NMJ vulnerability in SMNΔ7 mice (Fig. 7). Although most vulnerable muscles are predominantly fast-twitch, a few of them are composed of a mix of fast and slow fibers (e.g. semispinalis capitis). In addition, not all fast-twitch muscles are vulnerable. This is consistent with studies in a more severe SMA mouse model (Smn−/−;SMN2) which showed that both slow-twitch and fast-twitch muscles are vulnerable (18,23). These observations suggest that muscle fiber type is unlikely the sole determinant of NMJ vulnerability in SMA.

Aside from muscle fiber type, synapsing phenotypes, characterized as fast-synapsing (FaSyn) and delayed-synapsing (DeSyn) according to the pattern of NMJ assembly and plasticity, may also confer synapse vulnerability (35–37). Specifically, FaSyn muscle may be more vulnerable to SMA-induced synapse loss (18). However, we noticed that several FaSyn muscles (e.g. adductor longus and tibialis anterior) are resistant to denervation in SMNΔ7 mice (Fig. 7). Therefore, it is unlikely that the FaSyn phenotype determines muscle vulnerability. On the other hand, of all the DeSyn muscles studied in SMA mouse models (i.e. diaphragm, sternocleidomastoid and the rostral band of LAL), all were resistant to denervation. It is possible that the DeSyn phenotype may confer some level of resistance to denervation. However, whether all DeSyn muscles are resistant to denervation requires further confirmation.

Together, our findings suggest that NMJ vulnerability in SMA is not simply attributed to a single determinant, but likely a combination of various risk factors involving both muscles and neurons. It will require several studies (e.g. gene array and transgenic mice) to reveal the detailed molecular mechanisms of selective vulnerability in SMA. Nonetheless, our extensive list of vulnerable and resistant muscles provides the foundation for future comparative studies, which could advance our understanding of selective vulnerability.

NMJs are formed but not maintained in SMNΔ7 mice

Our study of multiple time points throughout disease progression allowed us to explore the mechanisms of synaptic defects; specifically, whether NMJ denervation results from failures in synapse formation or maintenance.

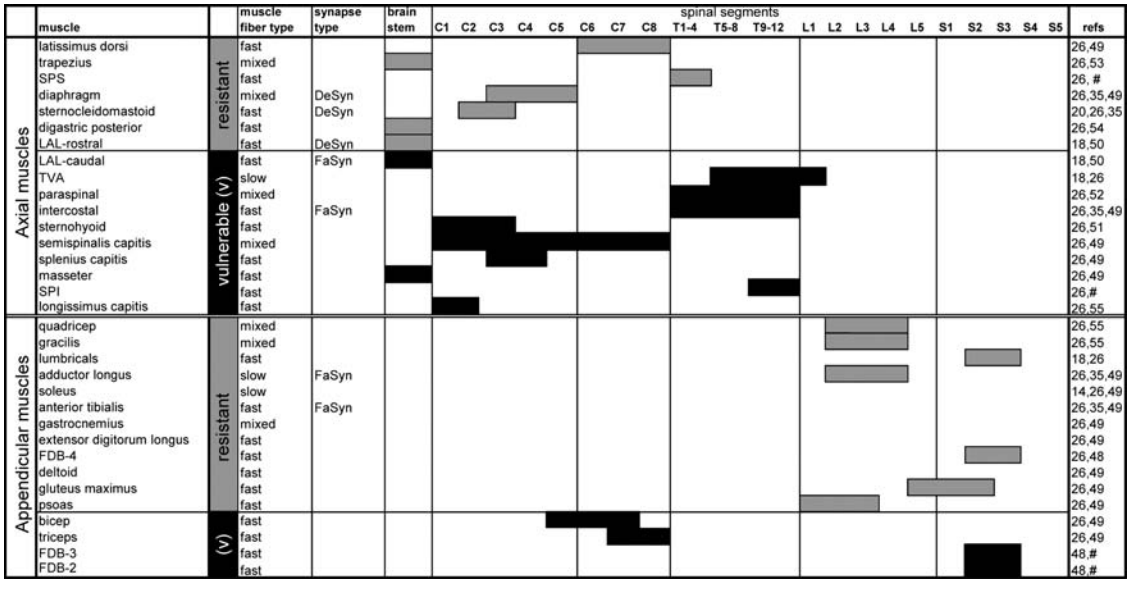

Figure 7. Summary of NMJ vulnerability in SMNΔ7 mice correlated with muscle locations, muscle fiber types, synapsing phenotypes and spinal origins of innervation. Axial and appendicular muscles listed as 'vulnerable' showed significant denervation in SMNΔ7 mice according to current and previous studies (in order of vulnerability). Muscles labeled as 'resistant' remained innervated even at the end stage of SMNΔ7 mice. The fiber type of a muscle was determined by the contents of slow (type I) and fast type (type IIa/b/x/d) fibers. Muscles composed of >75% slow type I fibers were here defined as 'slow'; muscles with <25% slow type I fibers were defined as 'fast'. Muscles containing between 25 and 75% slow type fibers were defined as 'mixed'. Muscle fiber types, synapsing types and spinal origin of innervation of the listed muscles were obtained from the following references: (18,20,26,35,48–55); #unpublished data.

Early developmental defects such as axon pathfinding have been shown to be involved in SMA pathogenesis in a zebrafish model of SMA (38). Our data, however, suggest that severe denervation in SMNΔ7 mice is unlikely attributed to developmental defects in target path-finding or initial synapse formation. First, initial nerve-muscle contacts were formed even in the severely denervated muscles of SMNΔ7 mice. Secondly, the number of presynaptic inputs per endplate in vulnerable muscles was similar in SMNΔ7 and control mice. These findings are consistent with observations in the more severe SMA model (Smn−/−;SMN2) (23,24) and suggest that the loss of NMJs in SMA mice is unlikely due to defects in synapse formation. Rather, failures in stabilizing NMJs in selective muscle groups may contribute to selective loss of NMJs in SMA.

What contributes to the loss of NMJs in SMA is unknown. One possibility is that defects in synaptic function may destabilize NMJs. Previous studies suggest that a reduction in synaptic transmission occurs in SMNΔ7 muscles (15,17,19). Although it is predictable that synapses would be functionally silent when synapses are physically lost, it would still be interesting to study if similar or more robust physiological defects also occur in vulnerable muscles preceding the loss of NMJs and motoneurons in SMA.

Another possibility contributing to the synapse loss is the disruption of cellular transport in motoneurons, which has been shown to cause denervation and neurodegeneration (39,40). Since neurofilament accumulation in diseased motoneurons can indicate disrupted cellular transport (41,42), it is possible that neurofilament accumulation at nerve terminals destabilizes NMJs, causing subsequent denervation in vulnerable muscles of SMNΔ7 mice. However, since we found equally prominent neurofilament accumulation in the nerve terminals innervating both vulnerable and resistant muscles in SMNΔ7 mice, it is unlikely that neurofilament accumulation causes denervation. Furthermore, neurofilament accumulation was also identified in muscles that are unaffected in SMA patients, such as the diaphragm (14). Although neurofilament accumulation in axonal swellings and at presynaptic terminals is a well-established pathological hallmark of SMA, the significance of this pathology in SMA is unknown. The specific cause of denervation thus remains elusive. Nevertheless, our findings suggest that defects in synapse maintenance may contribute to the mechanism of NMJ denervation.

It is important to note that, while the initial formation of NMJs was not impaired, NMJ denervation was observed in some muscles in embryonic ages (Fig. 3), which is consistent with previous observations in the severe SMA mice (24). These findings raise the possibility that early pathological changes already occur during embryonic development in SMA. Interestingly, recent studies have shown that early induction of SMN is more effective in rescuing SMA mice (43–45). Taken together, our findings provide further evidence for the importance of early therapeutic intervention that could effectively prevent disruption of NMJs in SMA.

Model system for preclinical studies

Our data demonstrated that NMJ denervation in clinically relevant muscles of SMNΔ7 mice was mitigated by effective postnatal drug (TSA) treatment. While survival and behavioral analyses offer important assays to assess drug efficacy in animal models, it is essential to also study drugs' effects on vulnerable targets of SMA. Showing that the NMJ is a vulnerable target and that NMJ denervation is amendable by

pharmacological intervention is an important finding because there are few available outcome measures to assess drug efficacy at the NMJ (46). One prevailing assay is measuring neurofilament accumulation at motor nerve terminals, but the functional significance of this synaptic pathology is unclear. In the more severe SMA mouse model (Smn−/−;SMN2), significant denervation in the intercostal and a caudal segment of levator auris longus muscle (18,24) could potentially serve as biomarkers for testing therapeutic efficacy *in vivo*. However, the use of this particular model for drug testing is limited by its short-lived nature. Therefore, the severe denervation in clinically relevant muscle groups in the milder SMNΔ7 mouse model shown in our study provides a convenient and sensitive outcome measure for evaluating drug efficacy at SMA NMJs. Furthermore, these muscles could be studied at multiple time points to assess whether candidate drug compounds could prevent denervation or facilitate re-innervation of NMJs.

In an effort to develop standard procedures for preclinical efficacy studies in SMNΔ7 mice, we present an extensive selection of highly vulnerable muscles useful for *in vivo* drug testing and therapeutic manipulation to correct neuromuscular dysfunction in SMA. The most severely denervated muscles with clinical relevance (e.g. SPI, splenius, longissimus), featuring easy dissection and unambiguous muscle location, serve as excellent preparations for *in vivo* drug efficacy studies. These muscles are flat and relatively thin, allowing quantification of all NMJs in whole-mount preparations. In addition, the most severely denervated appendicular muscles, FDB-2/3, are thin enough for imaging NMJs in whole-mount preparations and are easily accessible for local injection of drugs. Since both vulnerable (FDB-2/3) and resistant (FDB-4) muscle segments of the FDB are part of the same muscle, which are supplied by the plantar nerve, their similarity in location, innervation and function would serve as excellent preparations for understanding selective vulnerability to denervation in SMA.

Together, our systematic survey of NMJs in SMNΔ7 mice suggests that SMA involves defects in NMJ maintenance. Given the preferential vulnerability of NMJs in SMA, we believe that our data provide the basis of selecting appropriate neuromuscular preparations for addressing the mechanisms of synapse loss and selective vulnerability, and for evaluating therapeutic efficacy in SMA. Such studies are critical for advances in understanding the biology of synapse loss and finding effective treatments for SMA.

MATERIALS AND METHODS

Animals

All experimental procedures were carried out in compliance with the US National Institutes of Health Guide for the Care and Use of Laboratory Animals. The protocols were approved by the Institutional Animal Care and Use Committee of the University of Southern California (protocol #11136). Transgenic mice expressing SMA-like phenotypes were generated from breeder pairs obtained from The Jackson Laboratory (#5025; *FVB.Cg-Tg(SMN2*delta7)4299Ahmb Tg (SMN2)89Ahmb Smn1*^{tm1Msd}). YFP-SMNΔ7 mice were generated as previously described (17). Genotypes of transgenic mice were determined as described previously (16,47). Transgenic mice carrying either homozygous/heterozygous mouse *Smn* alleles were used as littermate controls.

Immunohistochemistry of NMJs

Mice of the desirable genotype and age were anaesthetized by IP injections of Nembutal (sodium pentobarbital; 50 mg/kg) or ketamine/xylazine (100 mg/kg ketamine/10 mg/kg xylazine) and transcardially perfused with Ringer's solution followed by 4% paraformaldehyde. Using whole-mount preparations, the following muscles were dissected and examined: latissimus dorsi, trapezius, serratus posterior superior, sternocleidomastoid, digastric posterior, intercostals, sternohyoid, semispinalis capitis, splenius capitis, masseter, SPI, longissimus capitis, gracilis, quadriceps femoris, lumbricals, FDB, deltoid, psoas, gluteus maximus, biceps brachii and triceps brachii. Thicker muscles (e.g. biceps, triceps, gluteus, quadriceps) were teased into layers of 5–10 fibers thick to facilitate penetration of antibodies that included: anti-neurofilament (1:2000; Chemicon) and anti-synaptophysin (1:200, Invitrogen) antibodies. AChRs were labeled with Alexa Fluor 594-conjugated α-bungarotoxin (Invitrogen). Fluorescently labeled NMJs were observed by epifluorescence or confocal microscopy. For imaging of NMJs, Z-stack images of immunostained whole-mount muscles were obtained at sequential focal planes 1 μm apart using the Zeiss LSM 510 META confocal microscope. Illustrated images are flattened projections of Z-stack images.

Quantification of innervation and pre-synaptic pathology

Innervation of muscles was quantified by visualization with an epifluorescence microscope equipped with a 40× objective. The innervation status of individual postsynaptic endplates was evaluated according to the extent to which the endplate overlaid with presynaptic components. Fully innervated endplates were defined by the complete overlap of presynaptic (i.e. synaptophysin) and postsynaptic (α-bungarotoxin) labeling. Partially denervated endplates were identified as only part of the endplate being covered by presynaptic labeling. Fully denervated endplates were devoid of any presynaptic labeling. For the multiple innervation analysis, the number of nerves (revealed by neurofilament immunostaining) innervating each endplate was counted under a ×100 objective. For assessment of presynaptic pathology, neurofilament accumulation at nerve terminals was quantified as neurofilament occupying >1/4 of the postsynaptic area. For each muscle sample, ∼200 endplates were evaluated from randomly selected visual fields of the whole mount. To achieve unbiased analyses, observers were blinded to the genotypes of muscles at the time of quantification. Data from three to five animals (for each genotype) were used for statistical analyses.

TSA treatment

TSA was purchased from Millipore (Billerica, MA, USA) and was dissolved in DMSO at a concentration of 10 μg/μl. Drug-treated SMNΔ7 mice were given TSA at an amount of 8 mg/

kg body weight and vehicle-treated SMNΔ7 control littermates were given an equal volume of vehicle (DMSO) by IP injection at a volume of 2.5 μl/g body weight. Injections were administered daily beginning from P1 and body weights were monitored daily prior to injections. TSA- and vehicle-treated animals in litters were maintained and fed by the mother until P12 when they were sacrificed for NMJ observation.

Statistical analysis

Data were statistically analyzed using two-tailed Student's *t*-tests with statistic software (Prism 5.0). $P < 0.05$ was considered significant. Results are expressed as mean ± SEM.

ACKNOWLEDGEMENTS

We thank members of the Ko laboratory for their critical comments on this manuscript.

Conflict of Interest statement. None declared.

FUNDING

This work was supported by National Institute of Health (grant number NS063296), Muscular Dystrophy Association, Spinal Muscular Atrophy Foundation and Families of Spinal Muscular Atrophy.

REFERENCES

1. Wee, C.D., Kong, L. and Sumner, C.J. (2010) The genetics of spinal muscular atrophies. *Curr. Opin. Neurol.*, **23**, 450–458.
2. Burghes, A.H. and Beattie, C.E. (2009) Spinal muscular atrophy: why do low levels of survival motor neuron protein make motor neurons sick?. *Nat. Rev. Neurosci.*, **10**, 597–609.
3. Meister, G., Buhler, D., Pillai, R., Lottspeich, F. and Fischer, U. (2001) A multiprotein complex mediates the ATP-dependent assembly of spliceosomal U snRNPs. *Nat. Cell Biol.*, **3**, 945–949.
4. Pellizzoni, L., Yong, J. and Dreyfuss, G. (2002) Essential role for the SMN complex in the specificity of snRNP assembly. *Science*, **298**, 1775–1779.
5. Feldkotter, M., Schwarzer, V., Wirth, R., Wienker, T.F. and Wirth, B. (2002) Quantitative analyses of SMN1 and SMN2 based on real-time lightCycler PCR: fast and highly reliable carrier testing and prediction of severity of spinal muscular atrophy. *Am. J. Hum. Genet.*, **70**, 358–368.
6. Monani, U.R. (2005) Spinal muscular atrophy: a deficiency in a ubiquitous protein; a motor neuron-specific disease. *Neuron*, **48**, 885–896.
7. McAndrew, P.E., Parsons, D.W., Simard, L.R., Rochette, C., Ray, P.N., Mendell, J.R., Prior, T.W. and Burghes, A.H. (1997) Identification of proximal spinal muscular atrophy carriers and patients by analysis of SMNT and SMNC gene copy number. *Am. J. Hum. Genet.*, **60**, 1411–1422.
8. Crawford, T.O. and Pardo, C.A. (1996) The neurobiology of childhood spinal muscular atrophy. *Neurobiol. Dis.*, **3**, 97–110.
9. Hausmanowa-Petrusewicz, I. and Vrbova, G. (2005) Spinal muscular atrophy: a delayed development hypothesis. *Neuroreport*, **16**, 657–661.
10. Lorson, C.L., Rindt, H. and Shababi, M. (2010) Spinal muscular atrophy: mechanisms and therapeutic strategies. *Hum. Mol. Genet.*, **19**, R111–R118.
11. Stavarachi, M., Apostol, P., Toma, M., Cimponeriu, D. and Gavrila, L. (2010) Spinal muscular atrophy disease: a literature review for therapeutic strategies. *J. Med. Life*, **3**, 3–9.
12. Swoboda, K.J., Prior, T.W., Scott, C.B., McNaught, T.P., Wride, M.C., Reyna, S.P. and Bromberg, M.B. (2005) Natural history of denervation in SMA: relation to age, SMN2 copy number, and function. *Ann. Neurol.*, **57**, 704–712.
13. Cifuentes-Diaz, C., Nicole, S., Velasco, M.E., Borra-Cebrian, C., Panozzo, C., Frugier, T., Millet, G., Roblot, N., Joshi, V. and Melki, J. (2002) Neurofilament accumulation at the motor endplate and lack of axonal sprouting in a spinal muscular atrophy mouse model. *Hum. Mol. Genet.*, **11**, 1439–1447.
14. Kariya, S., Park, G.H., Maeno-Hikichi, Y., Leykekhman, O., Lutz, C., Arkovitz, M.S., Landmesser, L.T. and Monani, U.R. (2008) Reduced SMN protein impairs maturation of the neuromuscular junctions in mouse models of spinal muscular atrophy. *Hum. Mol. Genet.*, **17**, 2552–2569.
15. Kong, L., Wang, X., Choe, D.W., Polley, M., Burnett, B.G., Bosch-Marce, M., Griffin, J.W., Rich, M.M. and Sumner, C.J. (2009) Impaired synaptic vesicle release and immaturity of neuromuscular junctions in spinal muscular atrophy mice. *J. Neurosci.*, **29**, 842–851.
16. Le, T.T., Pham, L.T., Butchbach, M.E., Zhang, H.L., Monani, U.R., Coovert, D.D., Gavrilina, T.O., Xing, L., Bassell, G.J. and Burghes, A.H. (2005) SMNDelta7, the major product of the centromeric survival motor neuron (SMN2) gene, extends survival in mice with spinal muscular atrophy and associates with full-length SMN. *Hum. Mol. Genet.*, **14**, 845–857.
17. Ling, K.K., Lin, M.Y., Zingg, B., Feng, Z. and Ko, C.P. (2010) Synaptic defects in the spinal and neuromuscular circuitry in a mouse model of spinal muscular atrophy. *PLoS ONE*, **5**, e15457.
18. Murray, L.M., Comley, L.H., Thomson, D., Parkinson, N., Talbot, K. and Gillingwater, T.H. (2008) Selective vulnerability of motor neurons and dissociation of pre- and post-synaptic pathology at the neuromuscular junction in mouse models of spinal muscular atrophy. *Hum. Mol. Genet.*, **17**, 949–962.
19. Ruiz, R., Casanas, J.J., Torres-Benito, L., Cano, R. and Tabares, L. (2010) Altered intracellular Ca2+ homeostasis in nerve terminals of severe spinal muscular atrophy mice. *J. Neurosci.*, **30**, 849–857.
20. Lee, Y.I., Mikesh, M., Smith, I., Rimer, M. and Thompson, W. (2011) Muscles in a mouse model of spinal muscular atrophy show profound defects in neuromuscular development even in the absence of failure in neuromuscular transmission or loss of motor neurons. *Dev. Biol.*, **356**, 432–444.
21. Mentis, G.Z., Blivis, D., Liu, W., Drobac, E., Crowder, M.E., Kong, L., Alvarez, F.J., Sumner, C.J. and O'Donovan, M.J. (2011) Early functional impairment of sensory-motor connectivity in a mouse model of spinal muscular atrophy. *Neuron*, **69**, 453–467.
22. Park, G.H., Maeno-Hikichi, Y., Awano, T., Landmesser, L.T. and Monani, U.R. (2010) Reduced survival of motor neuron (SMN) protein in motor neuronal progenitors functions cell autonomously to cause spinal muscular atrophy in model mice expressing the human centromeric (SMN2) gene. *J. Neurosci.*, **30**, 12005–12019.
23. Murray, L.M., Lee, S., Baumer, D., Parson, S.H., Talbot, K. and Gillingwater, T.H. (2010) Pre-symptomatic development of lower motor neuron connectivity in a mouse model of severe spinal muscular atrophy. *Hum. Mol. Genet.*, **19**, 420–433.
24. McGovern, V.L., Gavrilina, T.O., Beattie, C.E. and Burghes, A.H. (2008) Embryonic motor axon development in the severe SMA mouse. *Hum. Mol. Genet.*, **17**, 2900–2909.
25. Avila, A.M., Burnett, B.G., Taye, A.A., Gabanella, F., Knight, M.A., Hartenstein, P., Cizman, Z., Di Prospero, N.A., Pellizzoni, L., Fischbeck, K.H. *et al.* (2007) Trichostatin A increases SMN expression and survival in a mouse model of spinal muscular atrophy. *J. Clin. Invest.*, **117**, 659–671.
26. Hansen, J.T. and Lambert, D.R. (2008) Netter's Clinical Anatomy. Saunders Elsevier, Philadelphia.
27. Betz, W.J., Caldwell, J.H. and Ribchester, R.R. (1980) Sprouting of active nerve terminals in partially inactive muscles of the rat. *J. Physiol.*, **303**, 281–297.
28. Sanes, J.R. and Lichtman, J.W. (2001) Induction, assembly, maturation and maintenance of a postsynaptic apparatus. *Nat. Rev. Neurosci.*, **2**, 791–805.
29. Coers, C. and Woolf, A.L. (1959) *The Innervation of Muscle: A Biopsy Study*. Thomas, Springfield, IL.
30. Baumer, D., Lee, S., Nicholson, G., Davies, J.L., Parkinson, N.J., Murray, L.M., Gillingwater, T.H., Ansorge, O., Davies, K.E. and Talbot, K. (2009) Alternative splicing events are a late feature of pathology in a mouse model of spinal muscular atrophy. *PLoS Genet.*, **5**, e1000773.

31. Monani, U.R., Sendtner, M., Coovert, D.D., Parsons, D.W., Andreassi, C., Le, T.T., Jablonka, S., Schrank, B., Rossoll, W., Prior, T.W. *et al.* (2000) The human centromeric survival motor neuron gene (SMN2) rescues embryonic lethality in Smn(−/−) mice and results in a mouse with spinal muscular atrophy. *Hum. Mol. Genet.*, **9**, 333–339.
32. Fischer, L.R., Culver, D.G., Tennant, P., Davis, A.A., Wang, M., Castellano-Sanchez, A., Khan, J., Polak, M.A. and Glass, J.D. (2004) Amyotrophic lateral sclerosis is a distal axonopathy: evidence in mice and man. *Exp. Neurol.*, **185**, 232–240.
33. Frey, D., Schneider, C., Xu, L., Borg, J., Spooren, W. and Caroni, P. (2000) Early and selective loss of neuromuscular synapse subtypes with low sprouting competence in motoneuron diseases. *J. Neurosci.*, **20**, 2534–2542.
34. Hegedus, J., Putman, C.T. and Gordon, T. (2007) Time course of preferential motor unit loss in the SOD1 G93A mouse model of amyotrophic lateral sclerosis. *Neurobiol. Dis.*, **28**, 154–164.
35. Pun, S., Santos, A.F., Saxena, S., Xu, L. and Caroni, P. (2006) Selective vulnerability and pruning of phasic motoneuron axons in motoneuron disease alleviated by CNTF. *Nat. Neurosci.*, **9**, 408–419.
36. Santos, A.F. and Caroni, P. (2003) Assembly, plasticity and selective vulnerability to disease of mouse neuromuscular junctions. *J. Neurocytol.*, **32**, 849–862.
37. Xu, K., Jha, S., Hoch, W. and Dryer, S.E. (2006) Delayed synapsing muscles are more severely affected in an experimental model of MuSK-induced myasthenia gravis. *Neuroscience*, **143**, 655–659.
38. McWhorter, M.L., Monani, U.R., Burghes, A.H. and Beattie, C.E. (2003) Knockdown of the survival motor neuron (Smn) protein in zebrafish causes defects in motor axon outgrowth and pathfinding. *J. Cell Biol.*, **162**, 919–931.
39. Hafezparast, M., Klocke, R., Ruhrberg, C., Marquardt, A., Ahmad-Annuar, A., Bowen, S., Lalli, G., Witherden, A.S., Hummerich, H., Nicholson, S. *et al.* (2003) Mutations in dynein link motor neuron degeneration to defects in retrograde transport. *Science*, **300**, 808–812.
40. LaMonte, B.H., Wallace, K.E., Holloway, B.A., Shelly, S.S., Ascano, J., Tokito, M., Van Winkle, T., Howland, D.S. and Holzbaur, E.L. (2002) Disruption of dynein/dynactin inhibits axonal transport in motor neurons causing late-onset progressive degeneration. *Neuron*, **34**, 715–727.
41. Julien, J.P. (1997) Neurofilaments and motor neuron disease. *Trends Cell Biol.*, **7**, 243–249.
42. Julien, J.P. (2001) Amyotrophic lateral sclerosis: unfolding the toxicity of the misfolded. *Cell*, **104**, 581–591.
43. Foust, K.D., Wang, X., McGovern, V.L., Braun, L., Bevan, A.K., Haidet, A.M., Le, T.T., Morales, P.R., Rich, M.M., Burghes, A.H. *et al.* (2010) Rescue of the spinal muscular atrophy phenotype in a mouse model by early postnatal delivery of SMN. *Nat. Biotechnol.*, **28**, 271–274.
44. Le, T.T., McGovern, V.L., Alwine, I.E., Wang, X., Massoni-Laporte, A., Rich, M.M. and Burghes, A.H. (2011) Temporal requirement for high SMN expression in SMA mice. *Hum. Mol. Genet.*, **20**, 3578–3591.
45. Lutz, C.M., Kariya, S., Patruni, S., Osborne, M.A., Liu, D., Henderson, C.E., Li, D.K., Pellizzoni, L., Rojas, J., Valenzuela, D.M. *et al.* (2011) Postsymptomatic restoration of SMN rescues the disease phenotype in a mouse model of severe spinal muscular atrophy. *J. Clin. Invest.*, **121**, 3029–3041.
46. Willmann, R., Dubach, J. and Chen, K. (2011) Developing standard procedures for pre-clinical efficacy studies in mouse models of spinal muscular atrophy: report of the expert workshop 'Pre-clinical testing for SMA', Zurich, March 29–30th 2010. *Neuromuscul. Disord.*, **21**, 74–77.
47. Feng, G., Mellor, R.H., Bernstein, M., Keller-Peck, C., Nguyen, Q.T., Wallace, M., Nerbonne, J.M., Lichtman, J.W. and Sanes, J.R. (2000) Imaging neuronal subsets in transgenic mice expressing multiple spectral variants of GFP. *Neuron*, **28**, 41–51.
48. Carlsen, R.C., Larson, D.B. and Walsh, D.A. (1985) A fast-twitch oxidative-glycolytic muscle with a robust inward calcium current. *Can. J. Physiol. Pharmacol.*, **63**, 958–965.
49. Delp, M.D. and Duan, C. (1996) Composition and size of type I, IIA, IID/X, and IIB fibers and citrate synthase activity of rat muscle. *J. Appl. Physiol.*, **80**, 261–270.
50. Erzen, I., Cvetko, E., Obreza, S. and Angaut-Petit, D. (2000) Fiber types in the mouse levator auris longus muscle: a convenient preparation to study muscle and nerve plasticity. *J. Neurosci. Res.*, **59**, 692–697.
51. McGuire, M., MacDermott, M. and Bradford, A. (2002) The effects of chronic episodic hypercapnic hypoxia on rat upper airway muscle contractile properties and fiber-type distribution. *Chest*, **122**, 1400–1406.
52. Regev, G.J., Kim, C.W., Thacker, B.E., Tomiya, A., Garfin, S.R., Ward, S.R. and Lieber, R.L. (2010) Regional Myosin heavy chain distribution in selected paraspinal muscles. *Spine (Phila Pa 1976)*, **35**, 1265–1270.
53. Richmond, F.J., Singh, K. and Corneil, B.D. (2001) Neck muscles in the rhesus monkey. I. Muscle morphometry and histochemistry. *J. Neurophysiol.*, **86**, 1717–1728.
54. Sano, R., Tanaka, E., Korfage, J.A., Langenbach, G.E., Kawai, N., van Eijden, T.M. and Tanne, K. (2007) Heterogeneity of fiber characteristics in the rat masseter and digastric muscles. *J. Anat.*, **211**, 464–470.
55. Vigneron, P., Bacou, F. and Ashmore, C.R. (1976) Distribution heterogeneity of muscle fiber types in the rabbit longissimus muscle. *J. Anim. Sci.*, **43**, 985–988.